CHAPTER 221

Dispersion of pollution in a Wave Environment.

R. Koole[1] & C. Swan[2].

Abstract.

This paper concerns the wave-induced mixing of a discharged contaminant, and presents the results of a two-part laboratory investigation in which both a two-dimensional and a three-dimensional jet were discharged beneath a series of progressive gravity waves. In each case the measured data is compared to an identical discharge in a quiescent ambient. This comparison suggests that the oscillatory wave motion generates a region of intense fluid mixing which cannot be predicted by the existing integral solutions. Comparisons with a Lagrangian model, first proposed by Chin (1988), highlights the importance of the "apparent" mixing associated with the wave-induced deflection of the jet-axis. This provides a convincing explanation for both the non-Gaussian distributions observed by Sharp (1986), and the multi-stage structure of the centre-line decay (Chyan et al., 1991). Furthermore, quantitative comparisons with the Lagrangian model suggest that in addition to the wave-induced deflection, the oscillatory motion produces a significant increase in the rate at which ambient fluid is entrained into the emerging jet.

1. Introduction.

The design of coastal outfalls, and in particular the estimate of pollutant concentrations, is usually based upon a simplified steady state or quasi-steady state analysis. In the near-field region, close to the outlet orifice, the velocity and concentration profiles are typically described by some form of integral solution based upon the concentration of mass, momentum and, where appropriate, species concentration. Although these solutions were originally developed for buoyant

[1] Research assistant & [2] Lecturer. Department of Civil Engineering, Imperial College of Science Technology and Medicine, London, United Kingdom. SW7 2BU.

discharges in a quiescent ambient (Morton et al., 1956), subsequent research has shown that they may also be applied to a range of quasi-steady flows. This extension of the existing theory is, however, only valid if the unsteadiness of the ambient fluid has a time-scale which is significantly larger than the time-scales of the turbulent fluctuations within the emerging jet. As a result, a quasi-steady solution (based upon a modified integral solution) may be used to describe the discharge of pollution in a tidal flow, but should not be used to model the near-field mixing which arises when pollution is discharged into a wave environment. In this latter case the typical wave periods are similar to the eddy time-scales (of the order of seconds), and consequently there may be significant coupling between the turbulent fluctuations and the unsteadiness of the surrounding flow.

Indeed, previous qualitative studies (Shuto and Ti (1974), Ger (1979), Sharp (1986) and Chyan et al. (1991)) suggest that the oscillatory motion associated with the propagation of the surface gravity waves has a significant effect upon the local mixing characteristics. In particular, the wave motion appears to produce a large increase in the dilution immediately downstream of the discharge orifice. This region, which is usually referred to as the "zone of flow establishment", is characterised in a quiescent ambient by a gradual transition from a top-hat velocity profile at the exit to an approximately Gaussian distribution further downstream. This latter state marks the beginning of the so-called "zone of established flow" within which the integral solutions are valid. Recent quantitative measurements presented by Chyan and Hwung (1994) and Koole and Swan (1994) have shown that the "zone of flow establishment" is considerably shortened by the wave motion; and that a region of intense fluid mixing arises, the characteristics of which cannot be predicted by the existing integral solutions.

For example, there is both qualitative (Sharp, 1986) and quantitative evidence (Chyan and Hwung, 1994) to suggest that in some circumstances the radial distribution of both the axial velocity and the "pollutant" concentrations are no longer Gaussian. These observations are interpreted as providing evidence for a new wave-induced mixing mechanism (referred to as the "wave tractive mechanism") which involves the "entrapment" of large volumes of uncontaminated (ambient) fluid into the central area of the jet. Furthermore, Chyan and Hwung (1994) conclude that the axial variation in both the centre-line velocities and the concentrations no longer follow a typical exponential decay. Indeed, they provide evidence of a multi-stage decay in which three specific mechanisms of wave-induced mixing are identified.

The present paper will consider the nature of the mixing processes within the near-field region, and will, in particular, examine the occurrence of non-Gaussian distributions within the "zone of established flow". Section 2 commences with a brief outline of the experimental apparatus in which two widely differing discharges were considered. The first concerns a two-dimensional, non-buoyant, jet discharged in a horizontal plane; while the second concerns a three-dimensional, buoyant (thermal) discharge orientated in a vertical plane. In both cases two sets of measurements were undertaken so that the mixing and dilution of the jet in a wave environment can be directly compared with an identical discharge in a quiescent ambient. In section 3 the velocity and temperature data are compared with both the existing integral solutions and a simplified Lagrangian model. This latter solution was first proposed by Chin (1988) and further developed by Koole and Swan (1994). Evidence to support the various wave-induced mixing mechanisms is examined, as is the multi-stage structure of the centre-line decay. Finally, some conclusions regarding the effectiveness of the additional wave-induced mixing are made, and the practical implications for outfall design assessed.

2. Experimental apparatus.

Case 1: Two-dimensional, non-buoyant jet.

The first experimental study was undertaken within a narrow wave flume located in the Civil Engineering Department's hydraulics laboratory at Imperial College. This facility has good optical access, and is equipped with a numerically controlled random wave paddle located at one end of the wave flume. A large block of poly-ether foam is positioned at the opposite end to provide passive wave absorption. Typical reflection coefficients within this facility are less than 3%. The tank is 25m long, 0.3m wide, and has a working depth of 0.7m. The two-dimensional jet was introduced through a horizontal slot ($D=1$cm) located at mid-depth at the downstream end of the wave flume (figure 1a). The present results correspond to an exit velocity of 0.75m/s, and include measurements undertaken within a quiescent ambient and beneath a progressive regular wave train in which the wave amplitude was 30mm, and the wave period 1.04s.

The resulting flow field was measured using a two component laser Doppler anemometer in a forward scatter configuration. A 35mW helium-neon laser was used to create a three beam arrangement with cross polarisation. This apparatus allows the simultaneous measurement of two velocity components within a measuring volume which was estimated to be 0.5mm^3. After seeding the flow with milk (added in the ratio of approximately 100ppm), a data rate in excess of 2kHz was achieved so that the velocity components could be sampled at 500Hz with a measuring accuracy of $\pm 2\%$. Further details of these experimental observations are given by Koole and Swan (1994).

Case 2: Three-dimensional, buoyant jet.

The second set of measurements were undertaken in a larger wave flume which is also located in the hydraulics laboratory at Imperial College. This facility is 65m long, 2.75m wide, and is also equipped with a numerically controlled random wave paddle. At the downstream end of this flume the wave energy is dissipated on a 1:20 sloping beach. Under the present test conditions (see below) this produced a reflection coefficient of 4%. The "pollutant" was introduced in the form of a hot water discharge, through a 1cm diameter nozzle located on the bed of the wave flume. The initial jet was orientated in a vertical direction, and was positioned along the centre-line of the wave flume some 25m downstream of the wave paddle (figure 1b).

1(a). Two-dimensional, non-buoyant jet.

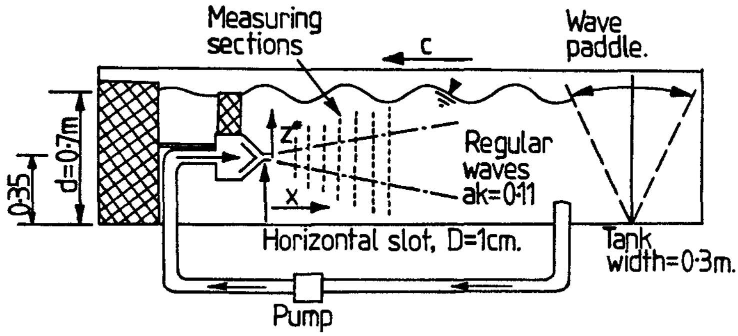

1(b). Three-dimensional, buoyant jet.

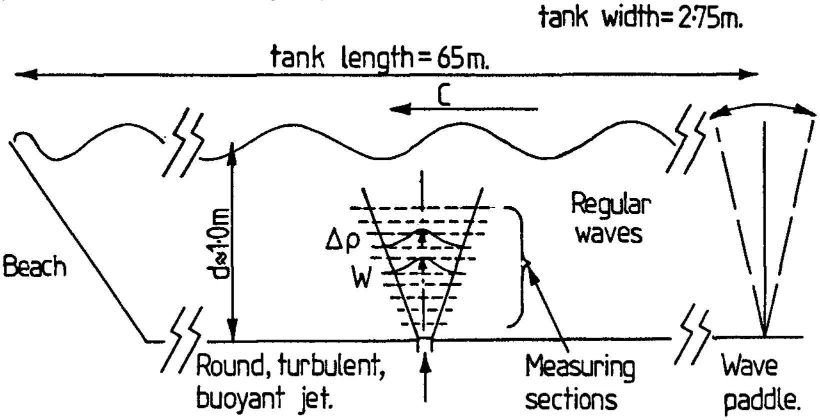

Figures 1a-1b. Experimental apparatus.

Although a wide range of test conditions were investigated, the present paper is only concerned with one specific data set in which the discharged "pollutant" was 35°C above the temperature of the ambient fluid. The results presented in section 3 correspond to an exit velocity of 0.55m/s. Once again, measurements were undertaken in a quiescent ambient, and beneath a progressive wave train in which the wave amplitude was 30mm and the wave period was 1.0s. Due to the restricted access and the physical dimensions of this facility a second laser Doppler anemometer was used to measure the velocity field. This system is based upon a 10mW helium-neon laser which is used to create a two beam arrangement from which one component of the flow field could be determined. The beams were passed down a fibre-optic cable, and emerged through a converging lens to focus 60mm from the fibre head. The intersection of the beams was observed in a back-scattered configuration. With careful seeding of the flow (using Trimiron Supersilk, MP-1005) an accuracy and data rate similar to that noted above were achieved. The temperature variations within the developing plume were measured using an array of 8 K-type thermocouples. These were manufactured at Imperial College using teflon coated wire with a diameter of 3 microns. Calibration tests indicated that these probes have an accuracy of $\pm 0.05^{\circ}C$ with a response time of 0.05s. This was sufficient to measure the temperature fluctuations within a wave cycle, and to assess the mixing and dilution of the jet at differing wave phases.

3. Measured data.

The axial velocity measured within the "zone of flow establishment" in Case 1 (described above) is shown on figures 2a-2b. In each of these figures, and many of the subsequent figures, two data sets are presented. The first, indicated by the open squares, corresponds to a discharge in a quiescent ambient; while the second, indicated by the solid triangles, corresponds to a discharge in the relevant wave conditions. Within the "zone of flow establishment" the mean jet velocity (U) in Case 1 is significantly larger than the wave-induced fluid motion (u,v), and thus there is little wave-induced displacement of the jet-axis. The experimental data presented on figures 2a-2b suggest that there is significant mixing of the jet immediately downstream of the nozzle, and that the "zone of flow establishment" (or the region over which a Gaussian distribution evolves) is significantly shortened. A similar pattern is observed in figures 3a-3b which describe the evolution of the three-dimensional discharge outlined in Case 2.

Figures 4a-4b concern Case 1, and present the variation in the axial velocity within the "zone of established flow" ($x > 5$cm). It is within this region that the integral solutions discussed previously are applicable. However, since the mean jet velocity is now of a similar magnitude to the wave-induced velocity (ie $U/v_{max} \approx 1$), the jet will undergo considerable lateral displacement. As a result the laboratory data, which corresponds to measurements undertaken at a number of points fixed in space and time-averaged over an integer number of wave periods (typically 40), will reflect both the dilution of the jet and its lateral displacement. In consequence, the velocity data gathered in a wave environment are very different from the integral solutions (indicated by a solid line on figures 4a-4b), whereas the measurements undertaken in a quiescent ambient are in good agreement with the existing theory. A similar sequence of results also arises in Case 2. In figures 5a-5b the average temperature profiles are presented within the so-called plume region (ie. that region of the flow where the buoyancy effects are important). Once again the influence of the wave motion is clearly apparent.

These results suggest that in both Case 1 and Case 2 the standard integral solutions are unable to describe the time-averaged laboratory data if the pollutant is discharged in a wave environment. However, the extent to which this change is due to the lateral displacement of the jet or the occurrence of additional wave-induced mixing remains unclear.

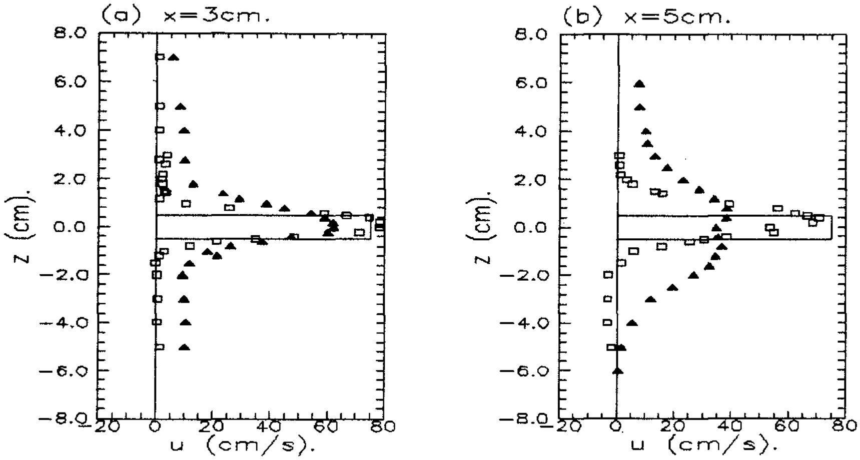

Figures 2a-2b. Case 1: axial velocity within the "zone of flow establishment".
□ Discharge in quiescent ambient, ▲ Discharge in waves.

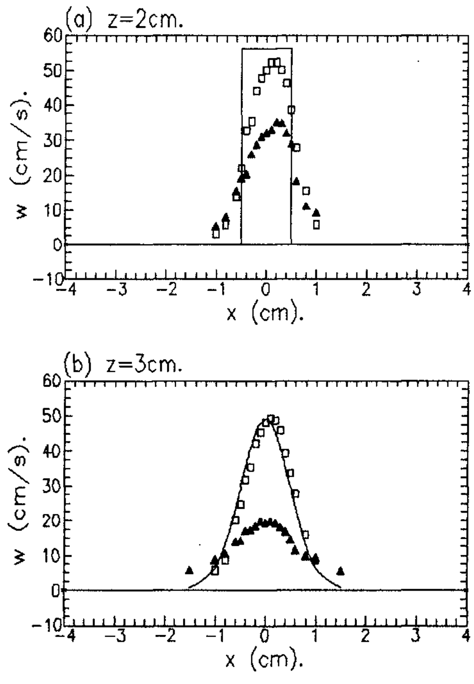

Figures 3a-3b. Case 2: axial velocity within the jet region.
□ Discharge in quiescent ambient, ▲ Discharge in waves.

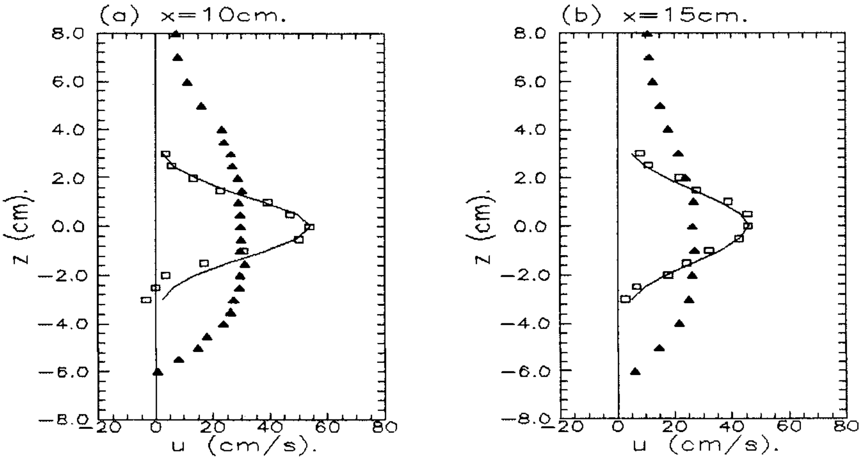

Figures 4a-4b. Case 1: axial velocity within the "zone of established flow".
□ Discharge in quiescent ambient, ▲ Discharge in waves.

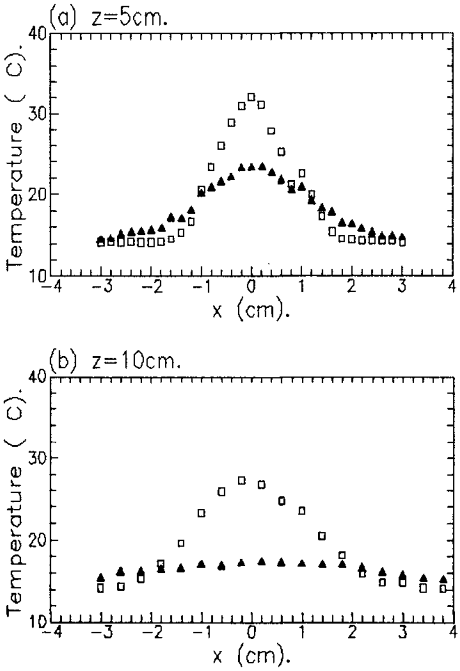

Figures 5a-5b. Case 2: temperature profiles within the plume region.
□ Discharge in quiescent ambient, ▲ Discharge in waves.

4. Discussion of Results.

To examine the relative importance of the jet displacement a simplified Lagrangian model similar to that proposed by Chin (1988) was adopted. This solution considers a succession of fluid elements discharged at regular intervals throughout a wave cycle. Each element is tracked, in both space and time, and the entrainment characteristics are based upon the velocity of the jet relative to the surrounding fluid. The conservation equations appropriate to Case 1 are given by:

$$\frac{\partial}{\partial \xi}\int_{-\infty}^{+\infty} U(\xi,\eta)\cos(\gamma)\,\partial\eta = 2\alpha U(\xi,0)\cos(\gamma)+\beta|\,U(\xi,0)\sin(\gamma)| \quad (1)$$

$$\frac{\partial}{\partial \xi}\int_{-\infty}^{+\infty}[\,U(\xi,\eta)\cos(\gamma)]^2\partial\eta = 0 \quad (2)$$

where (ξ,η) represent the local cartesian co-ordinates in which the $\eta=0$ corresponds to the instantaneous jet-axis, U is the velocity of the fluid element relative to the surrounding flow (figure 1a), and γ is the angle between U and the jet-axis. In Case 2 the conservation equations (including a heat flux relation) are best expressed in local polar co-ordinates (ξ,r), where the $\eta=0$ once again represents the instantaneous jet-axis:

$$\frac{\partial}{\partial \xi}\int_{0}^{\infty}2\pi r\rho(\xi,r)\,W(\xi,r)\cos(\gamma)\,\partial r = 2\pi b\rho_0\alpha W(\xi,0)\cos(\gamma) + 2b\rho_0\beta|\,W(\xi,0)\sin(\gamma)| \quad (3)$$

$$\frac{\partial}{\partial \xi}\int_{0}^{\infty}2\pi r[\,W(\xi,r)\cos(\gamma)]^2\rho(\xi,r)\,\partial r = \int_{0}^{\infty}2\pi r[\rho_0-\rho(\xi,r)]g\cos(\gamma)\,\partial r \quad (4)$$

$$\frac{\partial}{\partial \xi}\int_{0}^{\infty}2\pi r[W(\xi,r)\cos(\gamma)]T(\xi,r)\,\partial r = 0 \quad (5)$$

In this case W represents the velocity of the fluid element relative to the surrounding flow (figure 1b), $\rho(\xi,r)$ is the variable density within the jet, $T(\xi,r)$ is the corresponding temperature, and the subscript o refers to the ambient conditions within the surrounding fluid. In both cases (equations 1 and 3) α defines the coefficient of radial entrainment which is based upon the velocity component in-line with the instantaneous jet-axis ($U\cos(\gamma)$ or $W\cos(\gamma)$). In contrast, β is the coefficient of forced entrainment which defines the proportion of the laterally impinging flow ($U\sin(\gamma)$ or

Wsin(γ)) which is entrained.

Having identified an appropriate set of initial conditions, and made an assumption regarding the radial distribution of the velocity, density, and temperature, the conservation equations may be integrated to yield a Lagrangian solution for one fluid element released at a given phase of the wave cycle. If these calculations are repeated for a succession of fluid elements released at small increments of the phase angle, the resulting data may be time-averaged in the spatial domain to give a solution which is consistent with the laboratory measurements outlined above.

If the Lagrangian solution is based upon the entrainment coefficients appropriate to discharges in a quiescent ambient (ie. $\alpha=0.052$, $\beta=0$) a comparison with the existing integral solutions highlights the importance of the wave-induced displacement of the jet-axis. Calculations of this type suggest that there is significant wave-induced mixing. However, the reduction in the time-averaged velocities and/or concentrations does not in this case represent a "real" mixing process, but merely reflects the fact that under certain wave conditions the "pollutant" discharge only occupies some spatial locations for a small fraction of the wave cycle. Nevertheless, these results are important since they provide a qualitative explanation for two important features of the flow field which have been misinterpreted by previous researchers.

(a) The occurrence of non-Gaussian distributions.

Previous studies by Sharp (1986) and Chyan and Hwung (1994) have commented on the occurrence of "flat-topped" and, in particular, "bi-peaked" velocity and concentration profiles. These distributions have also been noted in the present study as indicated by the temperature data (Case 2) presented on figure 6. However, previous researchers have sought to explain this effect via an additional wave-induced mixing mechanism (referred to as an "enclosing mechanism") which involves the "entrapment" of ambient fluid within the interior of the jet. In contrast, the present calculations suggest that these non-Gaussian distributions may be directly explained by the lateral displacement of the jet and the time-averaged analysis of the data.

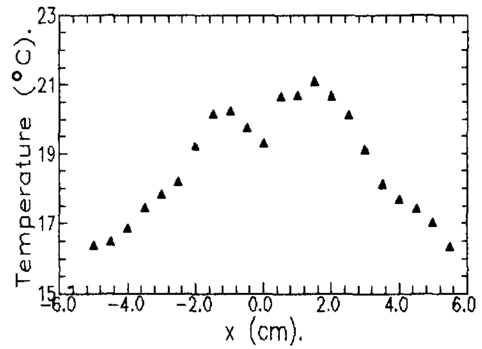

Figure 6. Radial variation in temperature data.

For example, if the length scale (l) of the wave-induced displacement is large in comparison to the width (b), the characteristics of the wave motion are such that the "residence-time" of the jet at any one spatial location increases with distance from the time-averaged centre-line. This may be demonstrated by considering the displacement of a Gaussian distribution at equal intervals throughout a wave cycle (Case 2 on figure 7a). This indicates that since the wave-induced horizontal velocity reduces to zero (as part of the cyclic reversal) at the extremities of the lateral displacement, the jet spends a larger proportion of one wave period at these locations. This, combined with the method of time-averaging in a fixed spatial domain (or, indeed, data collection from a probe fixed in space), produces a bi-peaked velocity and concentration profile (figure 7b). Furthermore, if the ratio of l/b is varied, then other non-Gaussian profiles such as the flat-topped velocity distributions shown on figure 7c may be explained.

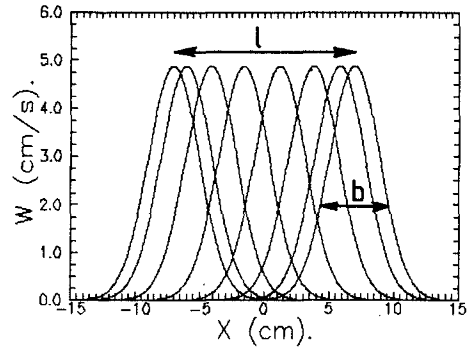

Figure 7a. Lateral displacement of a Gaussian distribution.

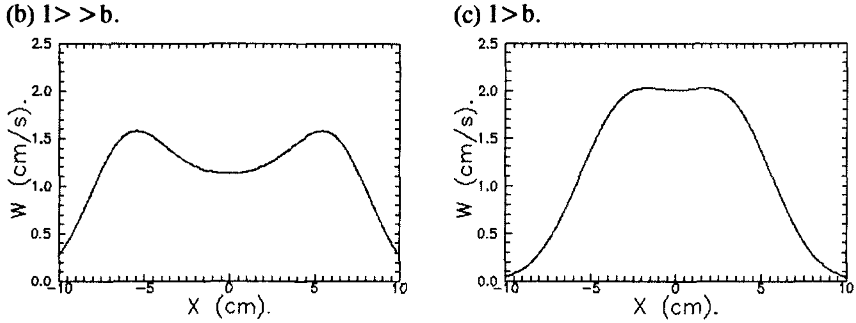

Figures 7b-7c. Time-averaged radial distributions.

(b) The structure of the centre-line decay.

If the time-averaged velocity and concentration data is measured along the mean jet-axis a decay curve similar to that indicated by the data points in figure 8 (Case 2) results. Once again, this pattern has been observed by previous researchers including Chyan et al (1991) and Chyan and Hwung (1994). Indeed, measurements of this type have been used to classify a three stage decay in which (with increasing distance from the nozzle) the so-called "deflection region" is characterised by a rapid dilution; the "transition region" by a steady or small rise; and the "developed region" by a gradual decay. Unfortunately, the nature of the mixing mechanisms within these layers remains unclear. In particular, no previous explanation has been offered for the increase in both the axial velocity and the pollutant concentrations with increasing distance from the nozzle (ie. within the "transition region").

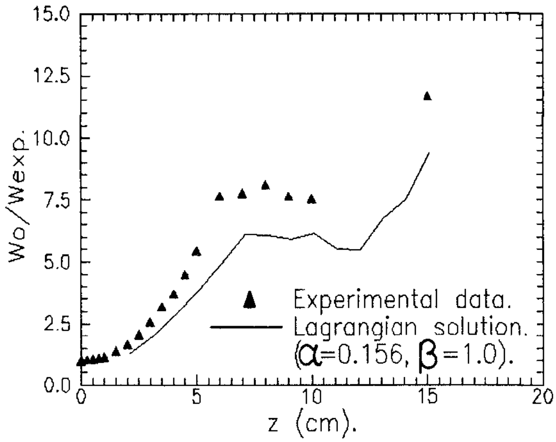

Figure 8. Decay of centre-line velocity (Case 2).

However, it is difficult to envisage how the dilution of the jet could in some way reduce (ie. for the fluid to effectively become un-mixed). As a result, a more probable explanation lies in a reduction in the "apparent" dilution. In other words, at some height above the nozzle, the wave-induced displacement of the jet-axis is reduced. The Lagrangian solution outlined above predicts exactly this effect. Figure 9 describes the trajectory of successive fluid elements released at equal intervals throughout a wave period. In this case, it is clear that the maximum lateral displacement of the fluid elements, and hence the maximum "apparent" dilution, occurs at a height of 12cm above the nozzle. Beyond this point the displacement first reduces and then increases. The present calculations suggest that this intermediate stage will produce an increase in both the predicted time-averaged velocity and concentration. Indeed, the solid curve indicated on figure 8 corresponds to the present Lagrangian solution. This appears to be in good qualitative agreement with the experimental data. In particular, it provides a convincing explanation for the multi-stage structure of the centre-line decay.

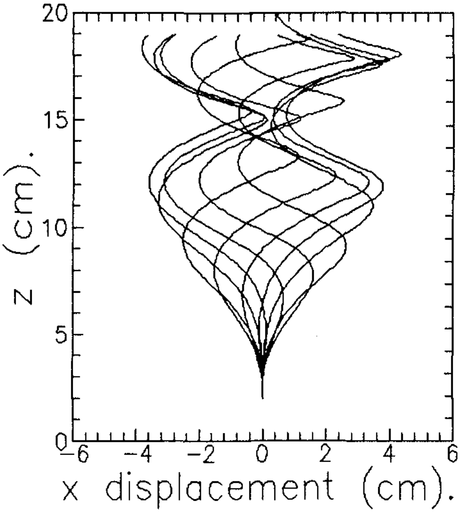

Figure 9. Trajectory of fluid elements (Case 2).

Unfortunately, good quantitative comparisons with the experimental data are, as yet, difficult to achieve because of the uncertainty in the entrainment coefficients (α and β). For example, the Lagrangian solution presented on figure 8 was based upon a three-fold increase in the coefficient of radial entrainment ($\alpha=0.156$). This suggests that in addition to the so-called "apparent" mixing (associated with the displacement of the fluid elements), the wave motion also produces a "real" increase in the dilution of the discharged pollutant. This point is further emphasised in figures 10a-10b. Figure 10a describes the mean centre-line velocity (Case 1), and compares the data with a number of potential solutions. The uppermost curve (indicated by a dashed line) represents an integral solution based upon the standard entrainment coefficients ($\alpha=0.052$ and $\beta=0$); while the second curve corresponds to a Lagrangian solution in which the forced entrainment is maximised ($\beta=1.0$), but the coefficient of radial entrainment remains unchanged ($\alpha=0.052$). The difference between these curves indicates the cumulative effect of the forced entrainment and "apparent" mixing. However, neither curve provides a good description of the experimental data. Indeed, a sensitivity study conducted by Koole and Swan (1994) showed that the best fit to the measured data was achieved by altering the initial conditions to shorten the "zone of flow establishment", and increasing the coefficient of radial entrainment to $\alpha=0.156$. This solution is presented on figure 10b. However, the present study (including the data presented on figure 8) suggests that these values ($\alpha=0.156$ and $\beta=1.0$) are not universally applicable. Indeed, the entrainment coefficients appear to be critically dependent upon the flow conditions at the discharge orifice. In particular, the relative balance between the momentum flux of the jet and that of the wave-induced motion at the discharge orifice appears to be very important.

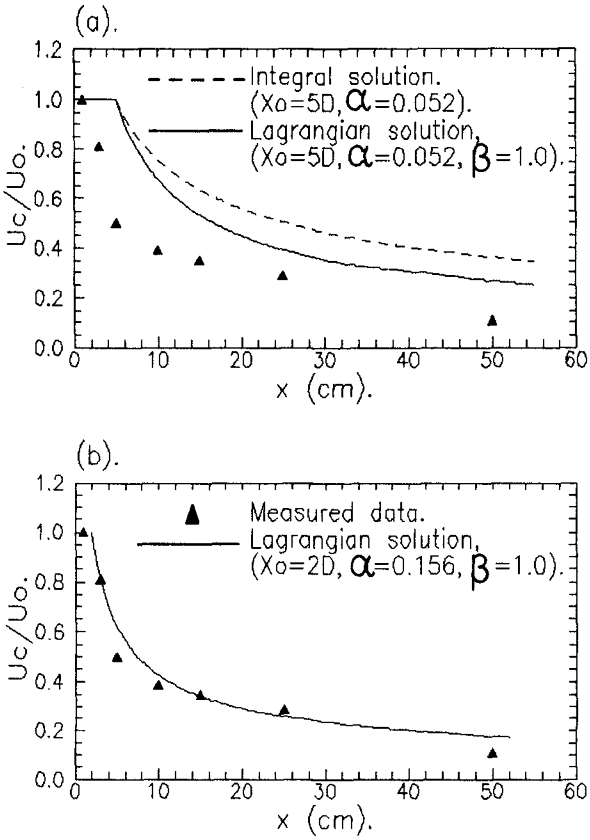

Figure 10a-10b. Non-dimensional centre-line velocity (Case 1).

5. Concluding remarks.

The present paper has presented the results of a two-part experimental study in which a two-dimensional non-buoyant jet (orientated in a horizontal direction), and a three-dimensional buoyant jet (orientated in a vertical direction) were discharged beneath a progressive regular wave train. In both cases the mean flow characteristics (including the temperature distribution in Case 2) were compared with an identical discharge in a quiescent ambient. These comparisons confirm that the oscillating wave kinematics have a significant effect upon the near-field mixing and dilution. In particular, the experimental data suggests that a region of intense fluid mixing arises immediately downstream of the discharge orifice, and that this results in a significant shortening of the "zone of flow establishment". This occurrence cannot be predicted by the existing integral solutions which form the basis of present near-field design calculations.

In contrast, a Lagrangian solution similar to that proposed by Chin (1988) provides a good qualitative description of the experimental data. In particular, it highlights the importance of the "apparent" mixing associated with the wave-induced displacement of the instantaneous jet-axis, and provides a plausible explanation for the non-Gaussian distributions of both the axial velocity and temperature. Indeed, it also explains the non-exponential decay of the mean centre-line characteristics. In particular, the apparent increase in both the velocity and concentration observed by previous authors (notable Chyan and Hwung, 1994) may be explained by the lateral displacement of the jet, and the time-averaged analysis of the laboratory data. Unfortunately, quantitative comparisons between the laboratory data and the Lagrangian solution are, as yet, difficult to achieve because of the uncertainty in the entrainment coefficients (α and β). However, the measurements suggest that in addition to the "apparent" mixing the wave motion also produces a significant increase in the rate at which ambient fluid is entrained into the jet. In the two-dimensional case a three-fold increase in the radial entrainment coefficient was recorded. However, comparisons with the three-dimensional data suggest that this increase is insufficient to predict the measured dilution. Indeed, it seems very unlikely that one universal entrainment coefficient will be applicable to all cases of wave-induced mixing.

Finally, although the present paper has only considered wave effects within the near-field region, one should not lose sight of the fact that these solutions provide the "initial" conditions for the random walk formulations used to calculate the dispersion of pollution in the far-field. As a result, the wave-induced mixing identified in the present paper may potentially have a significant effect upon the concentration contours predicted in the far-field.

Acknowledgements.

The authors gratefully acknowledge the financial support provided by the Engineering and Physical Sciences Research Council (EPSRC) under grant number GR/H/18999.

References.

Chin, D.A., 1988. Model of buoyant-jet surface-wave interaction. J. Waterway, Port, Coastal and Ocean Engng, ASCE, 114:331-345.

Chyan, J.M., Hwung, H.H. & Chang, Y.H., 1991. Wave effects on the mean flow characteristics of turbulent round jets. In: J.H.W. Lee and Y.K. Cheung (Editors), Environmental Hydraulics. Balkema, Rotterdam, The Netherlands. 1:109-114.

Chyan, J.M. & Hwung, H.H. 1994. On the interaction of a turbulent jet with waves. J. Hyd. Res. 31 (6): 791-810.

Ger, A.M., 1979. Wave effects on submerged buoyant jets. Proc. 8th Congress, Int. Ass. for Hyd. Res., New Delhi, India C:295-300.

Koole, R. & Swan, C. 1994. Measurements of a 2-D non-buoyant jet in a wave environment. Coastal Engineering, 24:151-169.

Morton, B.R., Taylor,G.I. & Turner, J.S., 1956. Turbulent gravitational convection from maintained and instantaneous sources. Proc. Roy. Soc., Series A, 234:1-23.

Sharp, J.J., 1986. The effects of waves on buoyant jets. Proc. Instn. Civ. Engrs., Part 2, 81:471-475.

Shuto, N. & Ti, L.H., 1974. Wave effects on buoyant plumes. Proc. 14th Inter. Conf. Coastal Eng., 2199-2209.